Journal of Materials Chemistry B

Accepted Manuscript

ROYAL SOCIETY OF CHEMISTRY

www.rsc.org/materialsB

Journal Name

Journal of Materials Chemistry B

Dynamic Article Links ►

Cite this: DOI: 10.1039/c0xx00000x

www.rsc.org/xxxxxx

ARTICLE TYPE

Mesoporous organosilica hybrids with a tunable amphoteric framework for controlled drug delivery

Madhappan Santha Moorthy,[a] Ji-Hye Park,[a] Jae-Ho Bae,[b] Sun-Hee Kim,[b] and Chang-Sik Ha[a]*

The chemical conversion of nitrile groups integrated in the pore wall frameworks of mesoporous organosilica hybrids (MSH) into either carboxylic acid groups or amine groups by acid or base hydrolysis method without altering mesostructural order is suggested. By this approach, bifunctional derivatives could be produced in the silica pore walls. The nitrile groups integrated covalently into the pore walls of the mesoporous organosilica hybrids were converted to reactive functionalities, such as carboxylic acid (–COOH) or amine ($–NH_2$) groups, by a treatment with H_2SO_4 or $LiAlH_4$ as the catalytic reagents. This facile approach allows the production of high amounts of either –COOH groups (3.26 mmol g^{-1}) or amine ($–NH_2$) groups (4.13 mmol g^{-1}) into the pore walls of the mesoporous organosilica hybrids. The synthesised materials were characterised by X-ray diffraction, N_2 sorption isotherms, Fourier transform infrared spectroscopy, transmission electron microscopy (TEM), scanning electron microscopy (SEM) and solid state ^{13}C cross-polarization magic angle spinning nuclear magnetic resonance spectroscopy (CP MAS NMR). Owing to the presence of hydrophilic basic diurea functional groups and –COOH or $–NH_2$ derivatives in the pore walls, the obtained samples could behave like bifunctional materials. The mesoporous organosilica hybrids with chemically derivatised carboxylic acid groups or amine functionalities in the pore wall frameworks were found to be suitable drug carriers for the controlled delivery of both hydrophilic (for example, 5-FU) and hydrophobic (e.g. IBU) drugs under an intracellular environment. The biocompatibility of the synthesised materials was also evaluated using a 3-(4,5-dimethylthiazol-2-yl)-2,5-diphenyltetrazolium bromide (MTT) assay. The cellular uptake was monitored by confocal laser scanning microscopy (CLSM). These results show that the synthesised materials have potential use as efficient carriers for drug delivery applications.

Introduction

Among the mesoporous silica materials,[1-6] mesoporous organosilica hybrids (MSH) is an important class of materials synthesised from bridged organosilane functional precursors [$(RO)_3$-Si-X-Si-$(RO)_3$] and inorganic silica.[7] Using this approach, a range of reactive organic functionalities can be introduced into the silica frameworks. Recently, mesoporous silica hybrids were used in nanobiotechnology and biomedical applications owing to their biocompatibility.[8] Despite the significant progress in using mesoporous silica materials as drug carriers, the controlled release of the loaded drugs is still a challenge.[9] Therefore, more research is needed to make their properties suitable for controlled drug delivery. Generally, for the controlled drug release in drug delivery applications, the surface properties of mesoporous silica materials require appropriate modifications with suitable functional groups. Thus far, the majority of the reported mesoporous silica hybrid materials were prepared using inert bridging groups, e.g. alkane, alkene and phenyl etc.[10] Nevertheless, their further chemical modification remains a significant challenge. The synthesis of mesoporous silica materials integrated with specific organic groups that can undergo further chemical modifications is an effective way of producing desired functional derivatives within the silica pore walls.[11] Thus, the prepared mesoporous organosilica could behave as bifunctionalised material. The suitable functional group incorporation in the silica pore walls and their further conversion by chemical hydrolysis treatment could be an effective approach over the multi-step post-surface modifications using commercially available functional precursors. Therefore, the desired functional groups can be introduced easily into the materials pore wall without altering the structural order of the material. The reactivity of the mesoporous silica materials can be improved significantly by increasing the number of active functionalities exposed in the materials. The integration of selective organic molecules into the mesoporous silica pore walls have several advantages over post-surface modification approach because the material can afford a high number of reactive functional moieties in the mesochannels due to the high loading of specific functional bridged units in the pore walls, uniform

[a] *Department of Polymer Science and Engineering, Pusan National University, Busan 609-735, Korea. E-mail: csha@pnu.edu*

[b] *Department of Biochemistry, School of Medicine, Pusan National University, Yangsan Hospital, Yangsan 626-870, Korea*

† Electronic supplementary information (ESI) available: N_2 adsorption-desorption isotherms, ^{13}C CP MAS NMR and TGA data of DU-MSH-CN, DU-MSH-COOH and DU-MSH-NH_2 materials.

functional group distribution, good control, and considerably reduced pore blockage and steric hindrance. Among the many ligand groups available, urea is an important hydrophilic ligand that has been used as a general acid catalyst for carbonyl compound activation.[12] The urea groups also play an important role in the self-assembly of functional materials due to hydrogen bonding interactions.[13] The N-H sites (-NH-CO-NH-) in the pore walls can act as binding sites for a range of guest molecules such as metal ions and drug molecules. Carboxylic acid (-COOH) groups are important functional groups in organic chemistry, owing to their ionisation/deprotonation behaviour in physiological and acidic/basic media. Mesoporous silica materials containing negatively-charged carboxylic acid groups are very useful for a variety of applications, such as acidic catalysts,[14] cationic species removal from aqueous solutions,[15] drug delivery[6b,16] and the immobilization of biomolecules.[17] Similarly, the amine group that contains a basic nitrogen atom with a lone pair of electrons is one of the most widely used functional groups for the surface modification of the mesoporous silica materials for a range of applications. Several efforts have been made to produce amine functionalised mesoporous materials for potential drug delivery. The functional groups containing mesoporous silica materials can adsorb high amount of drug molecules depends on the drug structure and more ordered and high degree of functionalized materials than the non-functionalized materials due to specific functional groups-drug interactions.[18] Owing to the strong interactions between drug molecules and the specific functional groups present in the carriers could be expected to show a sustained release rate than the non-functionalized materials.[18]

Considerable efforts have been made in the preparation of carboxylic acid[19] or amine groups[20] containing mesoporous silica materials either by surface modifications or co-condensation methods by using commercially available precursors (for example, carboxyethylsilanetriol sodium salt and amine precursors such as 3-aminopropyltriethoxysilane etc.). Nevertheless, the derivatization of carboxylic acid groups or amine groups into the mesoporous silica pore walls from the nitrile (-CN) moieties by chemical hydrolysis approach is remains an alternative approach. Such functional groups containing materials would be of great interest in adsorption, catalysis and drug delivery applications. The uptake and release behaviour of the drug molecules depend mainly on the content of reactive functional groups existed in the materials and the functional group-drug interactions in the drug delivery systems.[21] Enlargement of the pore size of the mesoporous silica carriers increased the drug adsorption capacity, whereas the mesoporous silica drug carriers synthesised using a co-condensation method was found to engross more drug molecules compared to surface modification method because of their more accessible mesospace, reduced steric hindrance and pore blockage than the latter case.[2,22] In this regard, mesoporous organosilica hybrids synthesised by co-condensation method possesses advantages such that the reactive organic functional groups occupy the pore walls, and induce rather low steric hindrance to allow easy accessibility to other guest molecules.[2] Reactive carboxylic acid groups or amine groups in the pore walls can interact with drug molecules. Therefore, the synthesis of the mesoporous materials with tunable pore wall properties is needed to produce the desired functional groups that can accommodate a range of drugs for controlled delivery. The main advantages of the incorporation of the bridged organosilane functional groups into the silica pore walls by co-condensation method is that the organo-functional precursors mostly located inside the pore walls with uniform distribution. By this way, the pore channels blockage and steric hindrance could be considerably reduced and therefore offered more space for loading/release of the guest molecules. On the other hand, in the post-surface modification method, specific functional units are modified onto the pore walls surfaces and the modified functional parts are facing towards the mesopore channels and there is more possibilities for mesopore blockage and steric hindrances due to the non-uniform distribution of the functionalities on the mesopore surfaces.

This paper reports the synthesis of mesoporous organosilica hybrid (MSH) materials with nitrile (-CN) functional groups that can be utilised further for chemical conversion to produce the reactive carboxylic acid or amine functionalities into the pore walls. A pair of functional groups, such as carboxylic acid-diurea or amine-diurea groups, were placed into the materials pore walls. For this purpose, a nitrile group-containing organic molecule was selected for the synthesis of mesoporous organosilica hybrids. In addition, the existing nitrile groups in the pore walls were converted chemically to active carboxylic acid groups by acid hydrolysis or amine groups by base hydrolysis approaches. These types of bi-/multifunctional groups containing mesoporous silica materials could be considered suitable for a range of potential applications, such as heavy metal adsorption, textile dye removal, and biomolecular and drug delivery applications. To demonstrate the potential applicability of the synthesised bifunctional organosilica hybrid material as a drug carrier, the loading and release of various therapeutic drugs were tested under different pH conditions using ibuprofen (IBU, a hydrophobic drug) and 5-fluorouracil (5-FU, a hydrophilic drug) as the model drugs. In addition, the biocompatible nature of the synthesised mesoporous organosilica drug carrier was also examined using a 3-(4,5-dimethylthiazol-2-yl)-2,5-diphenyltetrazolium bromide (MTT) assay. The intracellular internalization process of the prepared hybrid silica materials were evaluated by confocal laser scanning microscopy.

Experimental

Chemicals and reagents

Cetyltrimethylammonium bromide (CTAB), tetraethyl orthosilicate (TEOS), 3-(isocyanotopropyl)triethoxysilane (ICPTES), diaminomaleonitrile, sulphuric acid (H_2SO_4), lithium aluminium hydride ($LiAlH_4$), ibuprofen (IBU) and 5-fluorouracil (5-FU) were purchased from Aldrich Chemicals, USA. All chemicals were used as received.

Synthesis of bissilylated diurea-maleonitrile bridged organosilane precursor (DU-MN)

The diurea ligand groups were produced chemically by a reaction

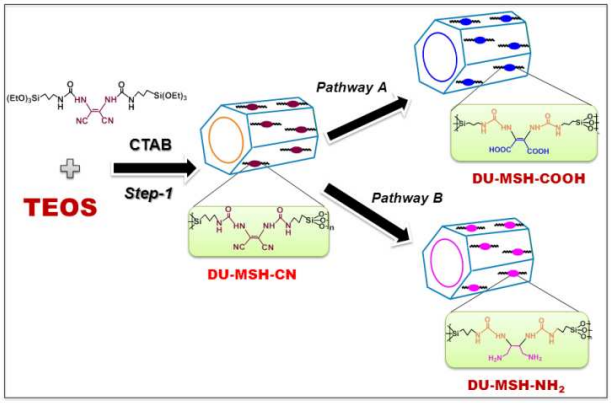

Scheme 1 Schematic diagram of synthetic pathways for DU-MSH-CN, DU-MSH-COOH and DU-MSH-NH_2 materials. DU-MN functional precursor-bridged mesoporous organosilica frameworks (step-1) and the formation of carboxylic acid groups (pathway A) and amine groups (pathway B) in the pore walls using acid or base hydrolysis methods.

of diaminomaleonitrile with 3-(isocyanotopropyl) triethoxysilane. Using this approach, the basic nature of the hydrophilic urea ligand groups can be introduced easily into the mesoporous silica pore walls. To synthesise the organosilane precursor, 0.25 g (2.5 mmol) of diaminomaleonitrile was dissolved in 25 ml of dry tetrahydrofuran (THF). To this, 1.25 g (5.02 mmol) of ICPTES was added and the reaction mixture was heated under reflux for 24 h in a N_2 atm. After the reaction was complete, the reaction mixture was concentrated under reduced pressure to obtain brown viscous oil as the product. The obtained product was purified with hexane and dried overnight in a vacuum at 40 °C. $[(EtO)_3Si(CH_2)_3NH\text{-}CO\text{-}NH]_2$-CNC=CCN, Yield: 95%; ^{1}H NMR (400 MHz, $CDCl_3$): δ 0.55 (t, 4H, $SiCH_2$), δ 1.2 (t, 18H, CH_3CH_2O), δ 1.62 (t, 4H, $SiCH_2CH_2$), δ 2.1 (t, 4H, CH_2NH_2), δ 3.4 (t, 8H, $NHCH_2$), δ 3.65 (q, 12H, CH_3CH_2O). ^{13}C NMR (400 MHz, $CDCl_3$): δ 7.8 ($SiCH_2$), δ 17.5 (CH_3), δ 25.6 (CH_2), δ 42.5 (CH_2N), δ 57.2 (CH_2O), δ 148.5 (C=O), δ 128.2 (C=C). FTIR (KBr): 1632 cm^{-1} (ν_{CO}), 2936, 2982 cm^{-1} ($\nu_{C\text{-}H}$), 2252 cm^{-1} ($\nu_{C\equiv N}$), 1538 cm^{-1} ($\nu_{N\text{-}H\ amide}$), 1436 cm^{-1} ($\nu_{N\text{-}C}$), 1248 cm^{-1} ($\nu_{Si\text{-}C}$).

The synthesis of the nitrile groups integrated diurea bridged mesoporous organosilica materials (DU-MSH-CN) and their further chemical conversion of the existed pore wall nitrile groups into either carboxylic acid groups or amine groups was achieved as follows.

Synthesis of diurea-containing mesoporous organosilica hybrids (DU-MSH-CN)

Mesoporous organosilica hybrid materials with a chemically tunable pore wall framework was synthesised conveniently using a nitrile group-containing diurea bridged organosilane precursor (DU-MN) using a co-condensation method. For typical synthesis, 1.0 g of CTAB was dissolved in 35 ml of deionised water containing 13 g of an ammonia solution (28%) and kept at room temperature for 30 min to obtain a clear solution with stirring. To this, a premixed solution of DU-MN precursor and TEOS were added slowly with vigorous stirring, and the final mixture was stirred for a further 24 h at 35 ºC and aged at 90 ºC for another 24 h to allow precipitation. A premixed solution of DU-MN and TEOS was added to make a DU-MN/DU-MN + TEOS mixture of 30 mol%. The molar composition of the reaction mixture was 1 (DU-MN + TEOS) : 0.125 CTAB : 69 NH_3 : 525 H_2O. The resulting product was filtered, washed with deionised water and dried overnight at 60 ºC. The surfactant was extracted from the material by treating them with a solution containing a mixture of ethanol (150 ml) and HCl (3 g, 36%) per gram of material at 60 ºC for 12 h. The procedure was repeated three times to allow complete removal of the surfactant from the material and dried in a vacuum, overnight at 60 ºC. The obtained product was labelled DU-MSH-CN (Scheme 1, Step-1).

Chemical hydrolysis of nitrile groups to carboxylic acid groups in the porewalls

The chemical conversion of integrated inert nitrile groups into active carboxylic acid groups was achieved conveniently using an acid hydrolysis process. For this purpose, a solution of sulphuric acid: glacial acetic acid (50:50) in 30 ml of water was placed in a reaction flask. To this, 0.2 g of the synthesised DU-MSH-CN samples was added and the mixture was heated under reflux using a condenser for 12 h. Subsequently, the suspension mixture was cooled to room temperature and 50 ml of deionised water was added and stirred for a further 1 h. Using this process, the pore wall nitrile groups were hydrolysed and converted to carboxylic acid groups. The obtained material was filtered, washed with deionised water until the filtrate become neutral, and dried at overnight 80 ºC.[23] The resulting material was labelled DU-MSH-COOH (Scheme 1, pathway A).

Chemical hydrolysis of nitrile groups to methylamine in the pore walls

The integrated nitrile groups into the pore walls of the DU-MSH-CN materials was converted to methylamine (-CH_2-NH_2) using a base hydrolysis approach in the presence of a catalytic amount of lithium aluminium hydride ($LiAlH_4$). A cold solution of $LiAlH_4$ (0.23 g, 14 mmol) in 15 ml tetrahydrofuran (THF) was added slowly to a reaction flask containing 0.2 g of the DU-MSH-CN samples in 25 ml of THF. The reaction mixture was stirred for 48 h at room temperature. Subsequently, the mixture was quenched with 10 ml of deionised water and stirred for a further 1 h at room temperature. The resulting mixture was neutralised with a 0.1 M NaOH solution (10 ml). After quenching, the resulting material was filtered, washed with ethanol, and dried overnight at 60 ºC.[24] During this reaction process, the nitrile groups underwent hydrolysis in the presence of a base catalyst and were converted to -CH_2-NH_2 groups. The obtained sample was labelled DU-MSH-NH_2 (Scheme 1, pathway B)

Preparation of dansyl chloride labelled 5-FU molecules

To trace the release of 5-FU molecules from the prepared silica carriers, 5-FU molecules were labelled with fluorescent dansyl chloride units as follows. About, 50 mg (0.18 mmol) of dansyl chloride was reacted with 25 mg (0.18 mmol) of 5-FU in EtOH (5 mL) in a flask and kept for stirring at 55 ºC for 24 h in the presence of Et_3N base under dark condition.[25] The obtained dansyl-labelled 5-FU was loaded into the prepared DU-MSH-COOH and DU-MSH-NH_2 materials and further utilized to monitor the cellular internalization by MCF-7 cells. In order to minimise the unconjugated species, an equimolar concentration (1:1) of 5-FU and dansyl chloride was used. The resulted solution was loaded into the materials. After loading, the sample was

thoroughly washed several times until the filtrate become colourless. By this way, the unconjugated dansyl chloride and 5-FU moieties were removed from the materials.

Preparation of FITC-labelled mesoporous silica carriers

The preconjugated N-1-(3-triethoxysilylpropyl)-N-fluorescenyl thiourea (FITC-APTES) was prepared by combining 5 μM of 3-aminopropyl triethoxysilane (APTES) and 2 mL of 5 μM of FITC ethanolic solution under continuous stirring under dark condition.[26] The synthesized DU-MSH-COOH and DU-MSH-NH_2 samples were labelled using FITC-APTES precursors by treating with 0.1 g of the prepared silica particles in ethanol solution was added 500 μL of FITC-APTES solution and stirred at 55 ºC for 12 h and then filtered, washed thoroughly with ethanol until the filtrate become colourless. The obtained samples were dried under 50 ºC, overnight under dark conditions.

Drug loading and release study

0.1 g of the carboxylic acid group-containing DU-MSH-COOH samples or amine group-containing DU-MSH-NH_2 samples, respectively, was loaded with IBU or 5-FU as the model drugs. The drug loading and release of IBU (5 mL, 15 mg mL^{-1}) drugs from the DU-MSH-COOH and DU-MSH-NH_2 samples was performed according to the reported procedure.[27,28] The loading process was performed using the respective solution of IBU in hexane or 5-FU in water (5 mL, 20 mg mL^{-1}) under sonication for 15 min and then the suspension was stirred for 24 h at room temperature. The drug-loaded samples were collected by centrifugation, washed with the minimum volume of hexane or water and dried in an oven at 50 °C. The amount of drug adsorbed by the samples was determined according to the change in concentration before and after adsorption using a UV-visible spectrometer (HITACHI 3220UV) at 272 nm for IBU and 265 nm for 5-FU. 102 mg g^{-1} of IBU and 93 mg g^{-1} of 5-FU was loaded respectively into the DU-MSH-COOH samples and 116 mg g^{-1} of IBU and 130 mg g^{-1} of 5-FU was loaded respectively into the DU-MSH-NH_2 samples. To evaluate the drug release behaviour of the materials, 100 mg of the IBU or 5-FU drug-loaded DU-MSH-COOH or DU-MSH-NH_2 samples was placed into a dialysis membrane bag (molecular weight cut off 5000 kDA) and immersed in 50 ml of a phosphate buffer solution (PBS). The pH of the release medium was adjusted to the desired pHs (pH 7.4 and 5.0) using a 0.1 M HCl/NaOH solution at 37 ºC with constant stirring at 150 rpm. 2 ml of the samples from the release medium were taken at given time intervals. The concentration of the drug released was measured by UV-visible spectroscopy at set times.

***In vitro* cytotoxicity test**

The *in vitro* cytotoxicity of the DU-MSH-COOH and DU-MSH-NH_2 samples was measured using human breast cancer (MCF-7) cells in an MTT assay. The MCF-7 cells were seeded at a density of $1x10^4$ cells per well in Dulbecco's modified Eagle's medium (DMEM) containing 10% foetal bovine serum (FBS, Gibco, Grand Island, USA), supplemented with 100 U mL^{-1} penicillin G and 100 μg mL^{-1} streptomycin in 96-well plates and incubated at 37 °C in a 5% CO_2/95% air incubator. To this, blank and 5-FU-loaded DU-MSH-COOH or DU-MSH-NH_2 samples dispersed in PBS solution (pH 7.4) at various concentrations (1, 10, 25 and 50 μg mL^{-1}) were added to the cells. To perform the control MTT assay test with pure 5-FU drugs, about 1, 10, 25 and 50 μL mL^{-1} of 5-FU drug solution was used from the specified concentration of stock 5-FU solution. After 24 h incubation, a MTT solution (5 mg mL^{-1} in PBS, 20 μL) was added to each well, and the cells were incubated for an additional 4 h at 37 °C. The medium was removed and dimethyl sulfoxide (DMSO, 200 μL) was added to each well to dissolve the MTT formazan crystals. The absorbance was measured using a microplate reader (Dynatech ELISA reader model MR 7000) at a wavelength of 570 nm. Three replicates were counted for each sample. The cell viability was calculated using the following equation:

$$\text{Cell viability ratio (\%)} = OD_{treated}/OD_{control} \text{ X } 100$$

where $OD_{treated}$ was obtained for the cells treated with the 5-FU-loaded DU-MSH-COOH and DU-MSH-NH_2 samples for 24 h. The $OD_{control}$ was obtained for the cells treated with the blank samples with the other culture conditions kept the same.

***In vitro* cellular uptake**

To monitor the pH responsive loading/release behaviour of the IBU or 5-FU drugs from the DU-MSH-COOH and DU-MSH-NH_2 samples, human breast cancer cells (MCF-7) were incubated with the dansyl-labelled 5-FU and Rhodamine B (Rh-B) (instead of the IBU drug) loaded samples, and cultured in DMEM containing 10% FBS (Gibco, Grand Island, USA), 100 units mL^{-1} penicillin, and 100 μg mL^{-1} streptomycin. The cells were maintained at 37 °C in humidified air containing 5% CO_2. The cells were seeded in a six-well plate at a density of 1×10^5 cells/well, and incubated in DMEM cell-culture media under 5% CO_2 at 37 °C for 6 h. The cell culture medium was removed, and the cells were incubated with 0.5 mL of fresh medium containing 25 μg of the dansyl-5FU or Rh-B loaded carrier particles. The cells were then incubated for a further 2 h. The cells were washed with PBS (pH 7.4, 0.1 M) and the intracellular release of encapsulated drugs was observed by confocal laser scanning microscopy (CLSM, Leica, TCS-SP2).

Characterization

Fourier-transform infrared (FTIR, JASCO FTIR4100) spectroscopy was carried on samples in KBr pellets. N_2 adsorption-desorption were performed on a Nova 4000e surface area and pore analyser at -196 °C. The samples were degassed at 120 °C under vacuum for 3 h prior to the measurements. The BET (Brunauer-Emmet-Teller) method was used to calculate the specific surface area. The pore size distribution curves were obtained from an analysis of the adsorption branch using the Barrett-Joyner-Halenda (BJH) method. X-ray diffraction (XRD, a Bruker AXN) was performed using Cu Kα radiation (λ = 1.5418 Å) in the 2θ range, 1.2-10°. The TEM images were collected on a JEOL 2010 operating at an acceleration voltage of 200 kV. SEM characterization was performed using a JEOL 6400 microscope operated at 20 kV. The particle size distributions in suspension were measured by dynamic light scattering on a Malvern Zetasizer Nano-ZS (Malvern Instruments). ^{13}C cross polarization magnetic angle spinning (CP MAS) nuclear magnetic resonance (NMR, Bruker DSX 400) spectroscopy was obtained using a 4 mm zirconia rotor spinning at 6 kHz (resonance frequencies of 100.6 MHz for ^{13}C CP MAS NMR; 90° pulse width of 5 μs, contact time of 2 ms, recycle delay of 3s). Thermogravimetric

analysis (TGA, Perkin-Elmer Pyris Diamond TG) was performed at a heating rate of 10 ºC min^{-1} in air. Confocal laser scanning microscopy (CLSM) images were obtained using a Leica (TCS-SP2) confocal fluorescence microscope.

Results and discussion

Scheme 1 presents a general overview of the synthesis method for the nitrile group integrated diurea bridged mesoporous silica hybrid material (DU-MSH-CN), and the further chemical conversion of the existing nitrile groups into the carboxylic acid groups or methylamine groups into the materials framework. First, the nitrile group-containing, diurea-bridged, mesoporous organosilica material was synthesised from a nitrile-bridged organosilane precursor (DU-MN) using a co-condensation method (Scheme 1, Step-1). Subsequently, the nitrile groups integrated in the mesopore walls were converted further to carboxylic acid groups or methylamine groups by acid hydrolysis (Scheme 1, pathway A)[23] or base hydrolysis (Scheme 1, pathway B).[24] These chemical conversions provided materials with surface derivatised carboxylic acid groups (DU-MSH-COOH) or amine groups (DU-MSH-NH_2) along with the existing diurea groups in the mesopore walls.

FTIR spectroscopy was used to confirm the integrated organosilane derivatives containing nitrile groups and diurea groups into the synthesised hybrid DU-MSH-CN samples as well as the chemically derivatised carboxylic acid groups and amine groups in the pore walls of the materials. Fig. 1(A(a,b)) shows the FTIR spectra of the nitrile groups-containing, diurea-bridged MSH materials (DU-MSH-CN) and carboxylic acid groups derivatised samples (DU-MSH-COOH). Fig. 1(B(a,b)) shows FTIR spectra of the DU-MSH-CN material and amine-derivatised mesoporous silica (DU-MSH-NH_2) material. In Fig. 1(A(a), B(a)), the peaks at 1637 cm^{-1} and 1482 cm^{-1} were assigned to the stretching vibrations of the C=O and N-H groups of the diurea.[29] Both materials showed peaks for C=C and -CN groups at 1458 cm^{-1} and 2232 cm^{-1}, respectively, indicating that the bridged ethylene carbon (C=C) and nitrile groups had been integrated into the materials pore wall.[30] All the materials showed the characteristic peaks at 2920 cm^{-1} and 2866 cm^{-1} that were assigned to the C-H stretching bands of alkyl carbon chains and broad absorption band at 1060-1200 cm^{-1}, indicating the formation of a Si-O-Si siloxane network. The stretching vibration peak at 963 cm^{-1} was attributed to residual silanol groups. After the respective chemical hydrolysis treatments, the stretching vibration peak for the sample was observed at 1718 cm^{-1} for the C=O vibrations of the carboxylic acid groups in the DU-MSH COOH samples, indicating the formation of –COOH groups by the acidic hydrolysis of –CN groups (Fig. 1(A(b)). Similarly, the DU-MSH-NH_2 sample showed a peak at 1393 cm^{-1}, indicating the presence of -NH_2 groups in the DU-MSH-NH_2 material produced by base hydrolysis of the existed -CN groups into methylamine (-CH_2-NH_2) in the DU-MSH-NH_2 pore walls (Fig. 1(B(b))). The stretching vibration peak was observed at 1362 cm^{-1} due to the presence of a -C=C- double bond in the DU-MSH-CN material. In contrast, the DU-MSH-NH_2 sample showed a ~26 cm^{-1} peak shift from 1362 cm^{-1} to 1388 cm^{-1} after being treated with $LiAlH_4$, indicating the reduction of a -C=C- double bond to a -C-C- single bond by catalytic hydrogenation using the $LiAlH_4$ catalyst (Fig. 1 (B(b))). It is notable that the stretching vibration peak is observed at 1362 cm^{-1} for the presence of -C=C- double bond carbon atoms in the DU-MSH-CN material. Meanwhile the DU-MSH-NH_2 sample shows the peak shift at about ~26 cm^{-1} from 1362 cm^{-1} to 1388 cm^{-1} after treating with $LiAlH_4$ indicating the reduction of -C=C- double bond into -C-C- single bond by catalytic hydrogenation occurred by $LiAlH_4$ catalyst (Fig. 1 (B(b))). Moreover, all other stretching peaks for the N-H groups at 1487 cm^{-1} and the peak at 1646 cm^{-1} for the -C=O groups revealed the existence of a bridged organic functional part in the pore wall framework of the DU-MSH-NH_2 materials. In addition, after the hydrolysis process, the prominent nitrile peak for both DU-MSH-COOH and DU-MSH-NH_2 at 2234 cm^{-1} disappeared, which clearly shows that the majority of the nitrile groups had been converted to either –COOH groups or –NH_2 groups, respectively with respect to the acid or base hydrolysis process catalysed by either H_2SO_4 or $LiAlH_4$.[31] The FTIR results confirmed the presence of integrated diurea groups and nitrile groups in the materials pore walls and its further chemical conversion of –CN groups to either -COOH groups or –NH_2 groups via an acid or base hydrolysis process. Fig. S1 (ESI†) shows the FTIR spectrum of the control sample mesoporous silica (MSN) that was prepared the same procedure without introducing any organic functional precursors. The obtained FTIR spectrum shows the stretching peaks at 1085 cm^{-1} and the peak at 953 cm^{-1} indicated the presence of Si–O–Si and surface Si–OH groups, respectively, in mesoporous silica sample implies that the absence of organic precursors in the controlled sample pore walls. Nitrogen sorption measurements were carried out to determine the mesoporosity of the synthesised materials. Fig. S2(A,B) (ESI†) presents the nitrogen adsorption-desorption isotherms and pore size distribution curves of the DU-MSH-CN, DU-MSH-COOH and DU-MSH-NH_2 samples.

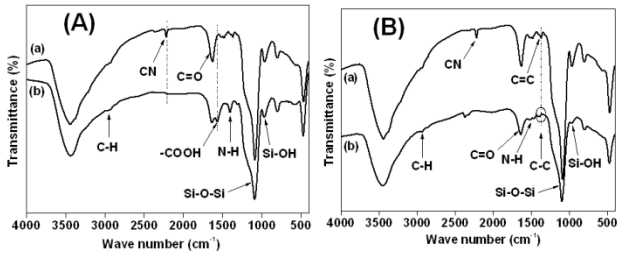

Fig. 1 FTIR spectra of (A) DU-MSH-CN (a) and DU-MSH-COOH (b) and (B) DU-MSH-CN (a) and DU-MSH-NH_2 (b) materials.

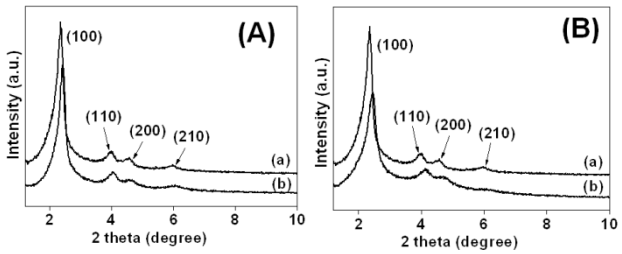

Fig. 2 Powder XRD patterns of (A) DU-MSH-CN (a) and DU-MSH-COOH (b) and (B) DU-MSH-CN (a) and DU-MSH-NH_2 (b) materials.

Table 1 Structural properties of the synthesized materials.

Sample	d_{100}/ nm[a]	S_{BET}/ m^2/g	Pore volume/ cm^3/g[b]	Pore diameter/ Å[c]	Functional groups content/mmol/g[d]	Drug loading/ mg/g	
						IBU	5-FU
DU-MSH-CN	3.70	672	0.36	21.2	4.80	65	74
DU-MSH-COOH	3.62	563	0.32	19.3	3.26	102	93
DU-MSH-NH_2	3.51	534	0.31	18.7	4.13	116	130

[a]Calculated from XRD analysis. [b]Calculated from the volume adsorbed with P/P_0 at 0.5. [c]Calculated from the adsorption branch of a nitrogen isotherm using the BJH model. [d]Calculated from TGA analysis and titration methods.

All samples exhibited type IV isotherms and H1 hysteresis, indicating the formation of mesostructural ordered materials with narrow pore size distributions. Table 1 lists the corresponding structural parameters. The DU-MSH-CN material exhibited a high surface area (S_{BET}) of 672 m^2g^{-1} and a mesopore volume of 0.36 cm^3g^{-1}. The surface areas and pore volumes of the DU-MSH-COOH and DU-MSH-NH_2 materials were lower than those of the DU-MSH-CN samples (Table 1). In addition, both DU-MSH-COOH and DU-MSH-NH_2 samples showed only a minor shift to a smaller pore diameter with slight peak broadening of the pore size distributions (inset in Fig. S2(A,B))) (ESI†) (Fig. S2(A(b),B(b))) see also Table 1). This highlights the formation of new functional –COOH and –NH_2 derivatives in the pore walls of the DU-MSH-COOH and DU-MSH-NH_2 samples. The results showed that the chemically-derived functional groups do not create considerable hindrance or pore blockage of the mesopore channels.

Fig. 2(A(a),B(a)) shows the low angle XRD patterns of the DU-MSH-CN materials. The XRD patterns revealed the main peaks at a low angle (100) 2.35º 2θ with a d-spacing of 3.7 nm. In addition, the second order (110), (200) and (210) peak reflections suggested the formation of a well-ordered hexagonal mesoporous silica network. After acid or base hydrolysis, all the materials exhibited similar XRD patterns to those before hydrolysis, even though the major diffraction peak intensities had decreased slightly for the materials DU-MSH-COOH (Fig. 2(A(b)) and DU-MSH-NH_2 (Fig. 2(B(b)) and (Table 1), indicating the formation of new functional derivatives into the pore walls of the materials by an acid/base hydrolysis process. The morphology and mesopore geometry of the DU-MSH-CN, DU-MSH-COOH and DU-MSH-NH_2 materials were analysed by SEM and TEM. Fig. 3(a1,b1,c1) shows SEM images of DU-MSH-CN, DU-MSH-COOH and DU-MSH-NH_2 materials. The samples showed short rod-like bended particles morphology with a mean particle size of approximately ~ 500 nm-1.5 µm (Fig. S3) (ESI†). Fig. 3(b1,c1) shows that the morphology of the particles was unaffected by the acid/base hydrolysis reaction conditions. Fig. 3(a2,b2,c2) presents TEM images of the DU-MSH-CN, DU- MSH-COOH and DU-MSH-NH_2 samples. All the materials clearly exhibited a hexagonal ordered mesostructure with uniformly ordered mesopores (Fig. 3(a2)). After acid or base hydrolysis process, the DU-MSH-COOH (Fig. 3(b2)) and DU-MSH-NH_2 (Fig. 3(c2)) materials showed uniformly aligned mesopore channel arrangements. TEM suggested that the ordered arrangement of the porous framework remained unchanged and the mesostructural order of the materials was unaffected by the acid or base hydrolysis reaction conditions. A comparison of the XRD patterns of the control sample MSN (Fig. S4) (ESI†) showed that MSN has distinct diffraction peaks corresponding to the [100], [110] and [200] planes, indicating that the sample has traditional mesoporous silica (MCM-41) type mesostructural arrangements.

The chemical transformations of the nitrile groups integrated into the carboxylic acid and amine groups, respectively, in the materials pore walls were confirmed by solid state NMR analysis. Fig. S5(a) (ESI†) shows the ^{13}C CP-MAS NMR spectra of the DU-MSH-CN materials. The spectrum of the DU-MSH-CN showed three resonance signals at 0 to 50 ppm, which were assigned to silicon-bridged propyl groups (-Si-CH_2-CH_2-CH_2-) and confirms the presence of Si-C bonds.[32] The carbon-resonance signals at 10.5 ppm, 22 ppm and 42.5 ppm were respectively assigned to the propyl carbon chains of –CH_2 bonded directly to a Si atom, -CH_2 group and –CH_2 group bonded directly to a –NH_2 group.[33] The resonance signals observed at 162 ppm and 56 ppm were assigned to C=O and C=C bonds, clearly indicating the existence of –C=C bridged DU-MN functionalities.[34] In addition, the two small peaks at 100 ppm and 135 ppm (market as asterisk) indicates the existence of a small fraction of surfactant residues. After hydrolysis, the resonance signal at 177 ppm was assigned to the C=O carbon atoms of the carboxylic acid groups (Fig. S5(b)) (ESI†). The presence of a small peak at 65 ppm indicates the existence of a small amount of unhydrolysed nitrile groups, and the peaks at 100 and 135 ppm, may be due to the residual surfactant fractions. Similarly, the DU-MSH-NH_2 sample showed propyl carbon resonance signals at 11.2 ppm, 20.6 ppm and 32.5 ppm for –CH_2 bonded directly to a Si atom, -CH_2 and -CH_2 bonded to –NH_2 groups, respectively. In addition, the new resonance signal at 72 ppm in the spectrum (Fig. S5(C)) reflected the formation of a –CH_2 group in -CH_2-NH_2 in the framework of the DU-MSH-NH_2 material obtained by the $LiAlH_4$-catalysed base hydrolysis of -CN to -CH_2-NH_2. Furthermore, a notable strong intense resonance signal at 105 ppm was assigned to the reduction of the -C=C- double bond to a -C-C- single bond from $LiAlH_4$-catalysed hydrogenation reaction during the base hydrolysis process. Furthermore, a resonance signal at 160 ppm for C=O groups and a small peak at 65 ppm indicates the presence of unhydrolysed nitrile groups. The ^{13}C CP MAS NMR spectra clearly show that -COOH and -CH_2-NH_2 groups had been produced successfully in the framework of the DU-MSH-COOH

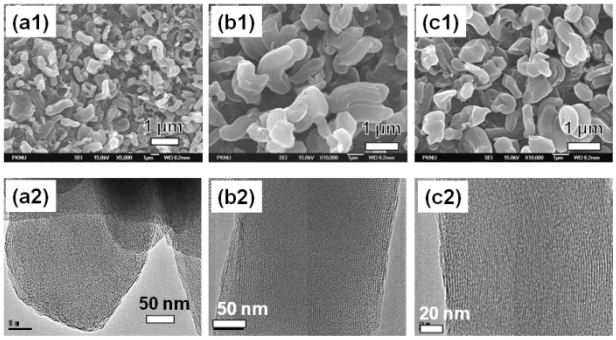

Fig. 3 SEM images of (a1) DU-MSH-CN (b1) DU-MSH-COOH and (c1) DU-MSH-NH_2, and TEM images of (a2) DU-MSH-CN (b2) DU-MSH-COOH and (c2) DU-MSH-NH_2 samples.

and DU-MSH-NH_2 materials from acid and base hydrolysis, respectively.

TGA was performed to estimate the amount of integrated DU-MN precursors into the pore walls of the DU-MSH-CN materials and its further derivatised –COOH and –NH_2 groups in the DU-MSH-COOH and DU-MSH-NH_2 samples. As shown in Fig. S6(A,B) (ESI†), all the materials showed a small amount of initial weight loss (~5 wt%) at 100 ºC due to the evaporation of physisorbed water or ethanol. The DU-MSH-CN sample showed the main weight loss of approximately 23 wt% in the temperature range, 101-650 ºC, indicating the decomposition of the integrated DU-MN organosilane precursor (Fig. S6(A(a),B(a))). In addition, the DU-MSH-COOH sample showed the additional weight loss of approximately 16 wt% occurred due to decomposition of the –COOH groups present in the materials pore walls (Fig. S6A(b)) (ESI†). Similarly, the DU-MSH-NH_2 sample showed the additional weight loss of approximately 12 wt%, indicating the decomposition of –NH_2 groups formed in the pore walls of the materials by the base hydrolysis process (Fig. S6B(b)) (ESI†). To confirm the presence of integrated organic functional units in the DU-MSH-COOH and DU-MSH-NH_2 samples, we have prepared a mesoporous silica sample as control without incorporate the organic functional units in the material. The TGA curve of the control MSN sample (Fig. S6(C) (ESI†) shows an initial weight is about ~5 wt.% indicates the evaporation of physisorbed water and there is no more considerable weight loss at higher temperature indicates the sample do not contains any organic functional parts in the materials.

Determination of the carboxylic acid and amine groups in the samples

The amount of carboxylic acid groups in the DU-MSH-COOH samples and amine groups in the DU-MSH-NH_2 samples were estimated by acid-base titration method according to reported procedure.[35] From the titration experimental values, the content of the carboxylic acid groups and amine groups were calculated accordingly to the following equation:

$$Am = 5C\ (V_1 - V_2) / m$$

where Am (mmol g^{-1}) represent the amount of carboxyl groups on DU-MSH-COOH, C (mol L^{-1}) is the calibrated concentration of 0.01 M HCl standard solution, V_1 (mL) is the consumed volume of the HCl standard solution titrating 20 mL (0.01 M) NaOH solution, V_2 (mL) is the consumed volume of the HCl standard solution titrating 20 mL of the supernatant, and m (g) is the mass of the used DU-MSH-COOH sample. The acid-base titration result shows that the content of the carboxyl acid groups in the DU-MSH-COOH sample was ca. ~3.26 mmol H^+/g. The amount of reactive carboxylic acid groups in the DU-MSH-COOH surfaces were determined by subtracting the value of acidic silanol groups in the DU-MSH-CN materials from the total value (~ 5.34 mmol H^+ g^{-1}) obtained from DU-MSH-COOH materials. The amount of calculated surface silanol groups in the DU-MSH-CN sample was ~ 2.08 mmol H^+ g^{-1}. Similarly, the concentration of the amine groups in the DU-MSH-NH_2 samples was calculated to be ~ 4.13 mmol H^+ g^{-1}. The titration results revealed that the amount of functional carboxylic acid and amine derivatives in the DU-MSH-COOH and DU-MSH-NH_2 samples contains relatively high amount of either carboxylic acid groups (3.26 mmol H^+ g^{-1}) or amine groups (4.13 mmol H^+ g^{-1}) in the materials pore walls than the reported –COOH groups containing materials[36] or –NH_2 modified materials[37] that were prepared by post-surface grafting approaches.

The development of a drug carrier system with unique properties has attracted significant attention in the field of drug delivery. A carrier system that can transport the effective dosage of drug molecules to the target site without premature release is an important prerequisite that impacts the therapeutic efficacy of drug delivery.[38] Among several drug delivery vehicles, mesoporous organosilica hybrid materials with the appropriate functionalities have been considered promising candidates for sustained and controlled drug delivery.[8a,39] Owing to the presence of specific organic functionalities, the system can accommodate large quantities of drug molecules in the mesoporous channels and allow better control of drug release depending on the intra/extra cellular stimuli. The drug molecules can interact with the carboxylic acid groups and diurea groups in the DU-MSH-COOH samples, and the amine groups and diurea groups in the DU-MSH-NH_2 materials in several ways (hydrogen bonding, electrostatic interactions, hydrophobic/hydrophilic interactions or ionic interactions). Ibuprofen (IBU), a hydrophobic anti-inflammatory drug, and 5-fluorouracil (5-FU), a hydrophilic anticancer drug, were chosen as model drugs to test the feasibility of DU-MSH-COOH and DU-MSH-NH_2 materials as an efficient drug carrier system to load and release a range of hydrophobic or hydrophilic drug molecules.

pH-dependent drug release

Fig. 4(A,B) shows the drug release profiles of IBU and 5-FU from either the IBU or 5-FU loaded DU-MSH-COOH or DU-MSH-NH_2 materials, respectively. The drugs, IBU/5-FU was loaded into the DU-MSH-COOH samples to evaluate the cooperative effects of the derivatised carboxylic acid groups and bridged diurea groups into the pore walls of the material in holding and releasing of drug molecules under different pH conditions. Fig. 4A(a,b) shows the drug release behaviour of the IBU or 5-FU loaded the DU-MSH-COOH samples under a range of pH conditions (pH 7.4 and 5.0). Fig. 4A(a) shows that the IBU release was considerably slow under acidic pH (pH 5.0), and only

~42 % of the drug molecules was released at 48 h release study. On the other hand, when the pH of the release medium was increased to pH 7.4, an enhanced IBU release was observed about ~86 % within 8 h and almost complete release at 48 h. This can be explained as follows. At lower pH (pH 5.0), the –N-H part of the urea groups (pKa = 0.2) becomes protonated. The protonated urea groups act as drug attraction centres to the carboxylic acid groups of IBU molecules (pKa = 4.43) via electrostatic/H-bonding interactions between the COOH parts of IBU molecules and the existing carboxylic acid derivatives (pKa = 3.7) and diurea groups in the DU-MSH-COOH samples, which results in a decreased release of IBU was observed. The –COOH groups of both in the IBU molecules and DU-MSH-COOH samples did not undergo ionisation/dissolution at lower pH,[40] whereas at higher pH (pH 7.4), the –COOH groups of the IBU molecules and in the DU-MSH-COOH samples became readily soluble and ionised to carboxylate ions ($–COO^-$). The ionised $–COO^-$ would increase an enhanced release of IBU from the DU-MSH-COOH samples at higher pH because strong electrostatic repulsion is expected between the ionised $–COO^-$ groups of the materials and the IBU drug molecules. Fig. 4A(b) shows the 5-FU release profiles from the 5-FU loaded DU-MSH-COOH samples. Under physiological pH (pH 7.4), the release of 5-FU (pKa = 8.2) was seems to partial release about ~47% at pH 7.4. This might be due to the strong hydrogen bonding/electrostatic interactions between the –N-H parts of diurea groups. In this stage, the –COOH groups may exist as $-COO^-$ ions due to ionisation at pH 7.4. On the other hand, at lower pH (pH 5.0) again a partial release of 5-FU was observed about ~67% at 48 h. The increased release of 5-FU at lower pH might be due to the strong electrostatic repulsion between the protonated N-H parts of the diurea groups in the DU-MSH-COOH materials and the 5-FU molecules.[41]

A similar set of drug release experiments were performed with the DU-MSH-NH_2 materials. Fig. 4B(a,b) shows the drug release behaviour of IBU/5-FU loaded DU-MSH-NH_2 samples at different pH (pH 7.4 and 5.0) at 37 ºC. The IBU-loaded DU-MSH-NH_2 system (Fig. 4B(a)) showed about 63 % at 8 h and further relatively a complete release of IBU about ~ 95% within 48 h at pH 7.4. The fast release was attributed to ionisation of the -COOH groups of IBU molecules under physiological pH. There is no considerable interactions existed between the ionised $-COO^-$ of IBU and the functional groups in the DU-MSH-NH_2 materials. On the other hand, under acidic pH (pH 5.0) conditions, lower release of approximately ~ 38% at pH 5.0. This was attributed to hydrogen bonding/electrostatic interactions between the protonated amine parts of the diurea groups (pKa = 0.2) in the DU-MSH-NH_2 samples and the IBU molecules. Furthermore, the poor solubility and hydrogen bonding interactions between DU-MSH-NH_2 and IBU molecules are responsible for the slow release of IBU molecules.[42] Fig. 4B(b) shows the 5-FU release profiles of the 5-FU loaded DU-MSH-NH_2 system. The 5-FU-loaded DU-MSH-NH_2 samples showed a considerable slow release (~ 28 %) under physiological pH. The formation of multiple hydrogen bonds between the -NH parts of the drug binding sites and 5-FU molecules is believed to be responsible for the slow release of 5-FU from the DU-MSH-NH_2/5-FU system under physiological pH. On the other hand, the amine groups (pKa = 10.6) and -NH parts of the diurea groups in the DU-MSH-NH_2 samples become readily protonated at lower pH and the 5-FU release was enhanced to ~90 % under reduced pH (pH 5.0). This was attributed to the relatively a strong repulsion between protonated amine/diurea groups of the drug binding sites in the DU-MSH-NH_2 samples and the 5-FU molecules at lower pH. All the systems showed a small initial burst release of IBU and 5-FU, which were attributed to the release of weakly bound physisorbed drug molecules inside/external surfaces of the materials. The drug release results clearly revealed the combined effects of the functional –COOH groups and diurea groups in the DU-MSH-COOH system or the combined effects of $–NH_2$/diurea groups in the DU-MSH-NH_2 systems. Moreover, the pH of the release medium had a strong influence on the IBU/5-FU released from either the DU-MSH-COOH or DU-MSH-NH_2 samples.

We evaluated the loading/release of IBU/5-FU from DU-MSH-CN samples to confirm the cooperative effect of bridged diurea groups on the adsorption/release of IBU and 5-FU drugs in the DU-MSH-COOH and DU-MSH-NH_2 samples. The calculated amount of the loaded IBU and 5-FU in the DU-MSH-CN sample was 65 mg/g of IBU and 74 mg/g of 5-FU, respectively. The amount of loaded IBU and 5-FU drugs in the DU-MSH-CN was relatively less than that the amount loaded in the DU-MSH-COOH and DU-MSH-NH_2 samples (see Table 1). We also examined the release behaviour of IBU and 5-FU from the DU-MSH-CN samples under pH 7.4 and 5.0, respectively (Fig. S7). As shown in Fig. S7(a), the release of IBU from the DU-MSH-CN samples shows about 95 % of IBU was released within 8 h under pH 7.4 condition, indicating the fast release of ionized IBU molecules at pH 7.4. Similarly, under acidic pH condition (pH 5.0) about 83 % of IBU was released out within 10 h. The enhanced release of IBU under acidic pHs is assumed due to the weak interactions of protonated amine parts of diurea groups and ionized carboxylate molecules. Fig. S7(b) shows the 5-FU release from the DU-MSH-CN samples. The 5-FU release profile shows that only about ~40 % of 5-FU molecules was released under pH 7.4 at 48 h. We assumed that the release of ~40 % 5-FU at pH 7.4 was attributed to the release of weakly interacted 5-FU molecules on the surface silanol groups. On the other hand, almost complete

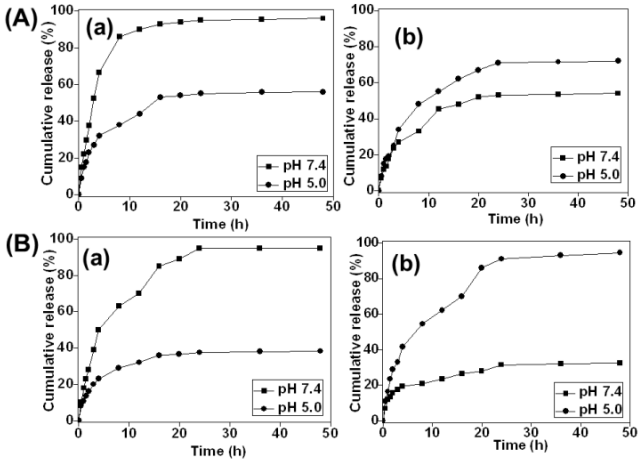

Fig. 4 Cumulative release of (a) IBU and (b) 5-FU from the DU-MSH-COOH (A) and DU-MSH-NH_2 (B) samples at different pH conditions (pH 7.4,and 5.0, respectively).

release of 5-FU was observed at pH 5.0. The complete release of 5-FU under acidic pHs may be due to the strong electrostatic repulsion between the protonated diurea groups and the 5-FU molecules. This study reveals that the bridged diurea groups could be also involved effectively in the loading/release of IBU/5-FU drugs in the DU-MSH-COOH and DU-MSH-NH_2 samples. The differences in the drug release behaviour might be due to the protonation and deprotonation behaviour of the carboxylic, amine and amide groups, also the pKa values of the functional groups and drug molecules.

We also examined the release of IBU and 5-FU drugs from the control MSN samples. Fig. S8(a) (ESI†) shows the release of IBU from MSN under pH 7.4 and 5.0, respectively. The observed drug release profiles seems the burst release rate is about > 95% of the loaded drugs were released within 10 h under both physiological and acidic pH conditions. This is because the IBU is hydrophobic molecules and the surface silanol groups in the MSN are hydrophilic and therefore a weak electrostatic interaction is expected between silanol groups and IBU molecules. The weak electrostatic/H-bonding interactions do not prevent the diffusion of the loaded drugs from the silica samples. Similar set of drug release experiment was performed with 5-FU drug under same pH conditions. The release of 5-FU from MSN samples is shown in Fig. S8(b) (ESI†). The 5-FU release from MSN at acidic conditions show enhanced burst release than the physiological pH condition. The burst release was observed under acidic conditions due to the protonation of 5-FU drugs and surface silanol groups and there is an electrostatic repulsion would be expected and thus make enhanced release under acidic pH conditions. On the other hand, under physiological conditions, the hydrophilic-hydrophilic/H-bonding interactions dominating because the hydrophilic nature of both 5-FU and surface silanol groups caused a slow release behaviour. IBU and 5-FU drugs loading in both materials could be divided into two parts in drug delivery kinetics. Some drug molecules get absorbed on the silica surfaces by weak physical absorption and might be released quickly, indicating the initial burst release. The rest of the IBU and 5-FU molecules which strongly interact with the existed carboxylic acid, amine and amide functionalities of the DU-MSH-COOH and DU-MSH-NH_2 materials via strong H-bonding/electrostatic interactions and thus caused slow release.

Several works have been reported about the surface interactions between the drugs and pure silica surfaces and functional group modified surfaces. The ionic interaction between the –COOH groups in IBU and the amino groups on the silica surfaces allow holding/release of IBU from the amine modified MCM-41 and SBA-15 materials. Both the modified functional groups and ordered structures play roles in influencing the adsorption amount of drugs on the surfaces. A higher loading of surface functional groups would generally lead to a higher loading of drugs than the unmodified materials.[43] Zhu et al.[44a] reported that the IBU molecules can be adsorbed on the pore surfaces by H-bonding interactions between carboxylic acid groups and surface silanol groups. Zheng et al.[44b] also observed that the adsorption of aspirin drugs by modified MCM-41 by H-bonding interactions of carboxyl groups and surface modified amine groups and surface silanol groups.[44] Babonneau et al.[45] studied the encapsulation of IBU molecules in the MCM-41 materials. The observed study reveals that the interaction between IBU molecules and silica surface is weak which favours the fast drug release from the materials. Zhu et al.[46] observed different aspirin drug release behaviour from the MCM-41 material and aminopropyl groups modified MCM-41 materials. The aminopropyl modified MCM-41 shows slow release of aspirin because of the strong interactions of aspirin with amine groups than the interactions of aspirin with the surface silanol groups in the unmodified MCM-41 materials. The amount of aspirin adsorption by the amine modified MCM-41 shows higher than the unmodified MCM-41.[46] Rosenholm et al.[47] studied the effect of solvent and the functional groups on drug loading in the material. The observed results revealed the increased interactions between the salicylic acid molecules and the modified amine functionalities on the carrier surface, which result in increasing the loading degree and control the release of salicylic acid due to strong carboxylic acid-amine interactions. The amount of modified aminosilanols showed more profound influence on the net surface charge under normal physiological conditions than that of the unmodified materials.

The drug release can be effectively controlled by surface functional group-drug interactions. For this purpose, various chemical groups were used that are able to interact with drug release through H-bonding or ionic or electrostatic interactions. Vallet-Regi et al.[48a] and Kawi et al.[48b] found that the surface functionalized MCM-41 and SBA-15 with amine groups as an effective method to control IBU release. These evidence also supported by Vallet-Regi.[48c] Sun et al.[48d] also reported the adsorption and release of famotidine drugs onto the carboxylic acid functionalized mesoporous silica materials. The reported studies so far indicate that the post functionalization (surface grafting) leads to better adsorption-release results than the condensation method.[48a,b] In contrary, Zhu et al.[49a] proposed some controversy in this topic. They stated that owing to a uniform functional groups distribution, well order, less-steric hindrance of the functional groups, a better drug delivery rate could be obtained with the materials prepared by using co-condensation approach, rather than post-surface modifications or solvothermal process.[49] In this study, we also observed the synthesis of masoporous silica materials by co-condensation method is more reliable for drug loading and controlled release of drugs and also noted that the content of the functional groups in the materials are very important for more amount of drug loading and sustained release of the loaded drugs to the target sites.

A two-step release model proposed by Andersson which was based on Higuchi model.[50] Based on Fick's law, the equation of Higuchi model used to predict the drug release from DU-MSH-COOH and DU-MSH-NH_2 samples using following equation.

$$M_\infty = K_t\ 1/2\ M_t/M_\infty = K_t^{1/2}$$

where M_t is the drug released at time t, M_∞ is the quantity of drug released at infinite time, and K is the kinetic constant. K as the kinetic release constant is determined by the diffusivity of the drug in the solvent, porosity of the sample, total amount of drugs loaded in the sample and the solubility of the drug in the solvent used. From the drug release profile Fig. 4 (A(a,b) and B(a,b)) the

initial burst release step may be due to the release of physisorbed drugs in the sample surfaces and the second release step can be attributed to the release of loaded drugs that interacted with the existed –COOH, -NH2 and –CONH- sites in the materials. The kinetic plots exhibit good linearity ($r^2 > 0.97$) (Fig. S9(A(i,ii) and B(i,ii)) which indicates that the IBU and 5-FU diffusion and release from the DU-MSH-COOH and DU-MSH-NH_2 samples corresponds to Fick's law.

MTT assay analysis

The cytocompatibility of the DU-MSH-COOH and DU-MSH-NH_2 samples was evaluated further. Fig. 5 shows the *in vitro* cell viability of the blank and 5-FU loaded DU-MSH-COOH and DU-MSH-NH_2 samples to the MCF-7 cells at various concentrations (1, 10, 25 and 50 μg mL^{-1}). Both DU-MSH-COOH and DU-MSH-NH_2 without drug loading showed almost negligible cytotoxicity to MCF-7 cells under intracellular pH conditions (Fig. 5(a,b)) (blue bars). This shows that DU-MSH-COOH and DU-MSH-NH_2 are biocompatible. Fig. 5(a,b) (brown bars) shows the viability of the MCF-7 cells exposed to the 5-FU-loaded DU-MSH-COOH and 5-FU-loaded DU-MSH-NH_2 samples. The observed results show that the enhanced cytotoxicity to the MCF-7 cells. The cell toxicity increased with the concentrations of the 5-FU drugs that was released from the internalised 5-FU-loaded DU-MSH-COOH/DU-MSH-NH_2 samples into the MCF-7 cells (Fig. 5(a,b)(brown bars))). After 24 h incubation, the 5-FU-loaded DU-MSH-COOH system revealed enhanced cytotoxicity between 18 to 76 % with respect to the internalised concentration of the DU-MSH-COOH samples into the cells (Fig. 5(a)(brown bars). Similar effects were observed on the 5-FU loaded DU-MSH-NH_2 samples about ~25% to 82% cell toxicity (Fig. 5(d)(brown bars))). The enhanced cytotoxicity of the MCF-7 cells was caused due to the higher concentration of released 5-FU drugs from the internalised 5-FU-loaded DU-MSH-NH_2 samples into the MCF-7 cells. The DU-MSH-COOH and DU-MSH-NH_2 samples have more number of drug interacting –COOH and –NH sites, which may carry more numbers of 5-FU molecules that can be released to the MCF-7 cells due to the acidic intracellular medium and thus induce cell toxicity. For control experiment, the *in vitro* cytotoxicity of pure 5-FU drugs against MCF-7 cells was investigated by MTT assay. As shown in Fig. S10 (ESI†), the cell viability of the pure 5-FU drugs treated with MCF-7 cells showed about 95-57 % cell viability. As compared to the MTT results that obtained from the MCF-7 cells treated with 5-FU loaded DU-MSH-COOH and DU-MSH-NH_2 samples the control MTT result indicate that the less amount of 5-FU molecules were internalised by the MCF-7 cells under solution state. Thus, the cellular uptake of the DU-MSH- COOH and DU-MSH-NH_2 materials can carry more number of 5-FU drugs into the MCF-7 cells and release them under intracellular pH conditions and therefore is responsible for the enhanced cell toxicity about 25-87 % to MCF-7 cells than the pure 5-FU drugs (5-57%) with respect to the different concentrations (1, 10, 25 and 50 μL mL^{-1}, respectively) of in PBS solution (pH 7.4).

***In vitro* cellular uptake process**

Generally, large particle sizes are sometimes not reliable for cellular uptake process for the cells with small sizes. On the other hand, the particle size is about ~ 1 μm may suitable for the cells with comparatively large size such as MCF-7 cells (average diameter of 18 ± 2 μm)[51] and HeLa cells (average diameter of 10-30 μm).[52] The obtained results revealed that the MCF-7 cells can internalize DU-MSH-COOH and DU-MSH-NH_2 samples having the particle size range of 500 nm - 1.5 μm. But, the kinetics of the internalization may vary depends on the particle size. To visualize the cellular internalization of the DU-MSH-COOH and DU-MSH-NH_2 carriers, fluorescein isocyanate (FITC) was incorporated covalently into the silica walls by following the reported procedures.[53] To monitor the intracellular release of loaded drugs from the DU-MSH-COOH samples, we used Rh-B as model cargo for loading/release from the DU- MSH-COOH samples and dansyl-labelled 5-FU was used to monitor loading/release from the DU-MSH-NH_2 samples since the non-fluorescence behaviour of IBU and 5-FU drugs. Even though the Rh-B or dansyl-labelled 5-FU complex do not behave like pure IBU/5-FU drugs but we could see the intracellular release behaviour of IBU/5-FU from the DU-MSH-COOH or DU-MSH-

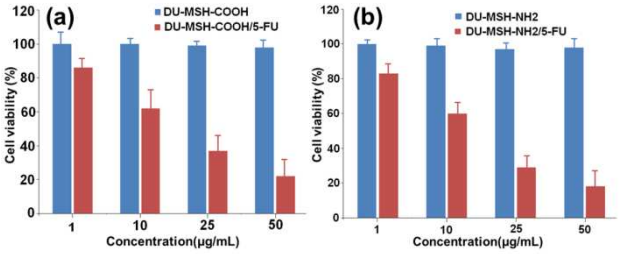

Fig. 5 *In vitro* cytotoxicity of the blank (a) DU-MSH-COOH and (b) DU-MSH-NH_2 (blue bars). In vitro cytotoxicity of the 5-FU-loaded (a) DU-MSH-COOH and (b) DU-MSH-NH_2 (brown bars), respectively.

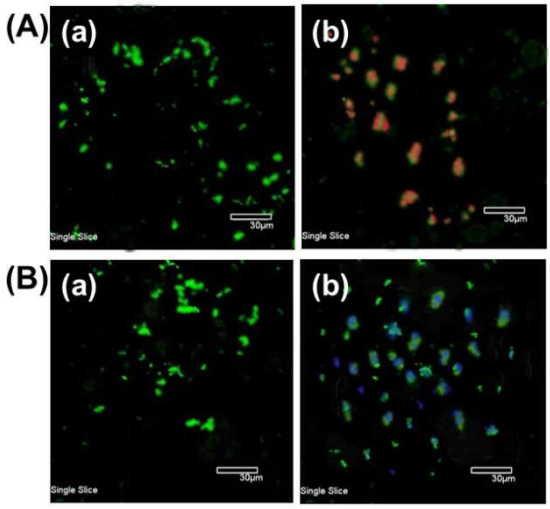

Fig. 6 Fluorescence visualization of the intracellular internalization of the (A) DU-MSH-COOH and (B) DU-MSH-NH_2 carriers. The MCF-cells were treated with FITC-labelled (A) DU-MSH-COOH and (B) DU-MSH-NH_2. Similarly, the MCF-cells were treated with Rh-B loaded DU-MSH-COOH (A(b)) and dansyl-labelled 5-FU loaded DU-MSH-NH_2 (B(b)). Scale bars correspond to 30 μm.

NH_2 samples under cellular pH of the cancer cells. Suspensions of Rh-B loaded DU-MSH-COOH and dansyl-labelled 5-FU loaded DU-MSH-NH_2 samples in PBS solution (pH 7.4) were introduced into the culture medium for 24 h. Fig. 6 A(a), B(a) shows the strong green fluorescence was observed into the cells indicating the internalization of DU-MSH-COOH and DU-MSH-NH_2 particles into the MCF-7 cells. In addition, the weak red fluorescence into the cells indicates the partial release of the Rh-B from the DU-MSH-COOH samples (Fig. 6A(b)). Similarly, the observation of the blue fluorescence indicating the release of loaded dansyl-labelled 5-FU from the DU-MSH-NH_2 samples under acidic pH conditions of the MCF-7 cell medium (Fig. 6B(b)). The confocal images reveal that the successful internalization of both DU-MSH-COOH and DU-MSH-NH_2 materials into the MCF-7 cells and the release of loaded cargos into the MCF-7 cellular medium.

Conclusions

In this work, we propose a new approach to produce either carboxylic acid or amine derivatives from the integrated nitrile functionalities by acid or base hydrolysis approaches. In the first step, mesoporous organosilicas was prepared using nitrile groups containing functional units. In the second step, acid or base hydrolysis were performed to produce carboxylic acid or amine derivatives from the existed nitrile groups in the pore walls. The successful preparation of the materials was confirmed by XRD, N_2 sorption isotherms and solid state ^{13}C MAS NMR analysis. The proposed approach is facile to produce more amounts of –COOH groups (3.26 mmol g^{-1}) and –NH_2 groups (4.13 mmol g^{-1}) in the materials pore wall frameworks without altering their mesostructural properties.

The utilization of the prepared materials as drug carrier for both hydrophilic and hydrophobic drugs was verified using 5-FU and IBU as model drugs under different pH conditions. We found that the drug release phenomena were well controlled by pH of the release medium. In addition, the MTT results revealed that the synthesized DU-MSH-COOH and DU-MSHNH_2 materials possess good biocompatible nature. Moreover, the confocal laser scanning microscopy images indicated that the prepared materials could be internalised by the MCF-7 cells even though the average particle size is relatively large about ~ 500 nm to 1.5 μm and the loaded drugs can be released under the cellular pH conditions of the MCF-7 cells. All the studied results suggest that the prepared mesoporous silica hybrid materials are suitable for biomedical applications.

Acknowledgements

The work was supported by the National Research Foundation of Korea through the Ministry of Science, ICT & Future Planning, Korea (Pioneer Research Center Program (No. 2013041888/201304889); Acceleration Research Program (No. 2013041172); Brain Korea 21 Plus program (21A2013800002)).

References

1 C.T. Kresge, M.E. Leonowicz, W.J. Roth, J.C. Vartuli and J.S. Beck, *Nature*, 1992, **359**, 710.

2 F. Hoffmann, M. Cornelius, J. Morell and M. Fröba, *Angew. Chem. Int. Ed*. 2006, **45**, 3216.

3 a) J.E. Lee, N. Lee, T. Kim, J. Kim and T. Hyeon, *Acc. Chem. Res*. 2011, **44**, 893; b) Z. Li, J.C. Barnes, A. Bosoy, J.F. Stoddart and J.I. Zink, *Chem. Soc. Rev*. 2012, **41**, 2590.

4 a) I. Rodriguez, S. Iborra, A. Corma, F. Rey and J.L. Jorda, *Chem. Commun*. 1999, 593; b) C.M. Crudden, M. Sateesh and R. Lewis, *J. Am. Chem. Soc*. 2005, **127**, 10045; c) X. Wang, Y. H. Tseng, C.C. Chan Jerry and S. Cheng, *Micropor. Mesopor. Mater*. 2005, **85**, 241.

5 a) S.Z. Qiao, C.Z. Yu, W. Xing, Q.H. Hu, H. Djojoputro and G.Q. Lu, *Chem. Mater*. 2005, **17**, 6172; b) A. Salis, D. Meloni, S. Ligas, M.F. Casula, M. Monduzzi, V. Solinas and E. Dumitru, *Langmuir*. 2005, **21**, 5511.

6 a) S.-W. Song, K. Hidajat and S. Kawi, *Langmuir*. 2005, **21**, 9568; b) Q. Yang, S. Wang, P. Fan, L. Wang, Y. Di, K. Lin and F.-S. Xiao, *Chem. Mater*. 2005, **17**, 5999; c) B.G. Trewyn, I.I. Slowing, S. Giri, H.-T. Chen and V.S.-Y. Lin, *Acc. Chem. Res*. 2007, **40**, 846; d) I.I. Slowing B.G. Trewyn, S. Giri and V.S.-Y. Lin, *Adv. Funct. Mater*. 2007, **17**, 1225.

7 a) R.J.P. Corriu, *Angew. Chem. Int. Ed*. 2000, **39**, 1376; b) S. Inagaki, S. Guan, Y. Fukushima, T. Ohsuna and O. Terasaki, *J. Am. Chem. Soc*. 1999, **121**, 9611; c) T. Asefa, M.J. MacLachlan, N. Coombs and G.A. Ozin, *Nature*. 1999, **402**, 867; d) B.J. Melde, B.T. Holland, C.F. Hanford and A. Stein, *Chem. Mater*. 1999, **11**, 3302.

8 a) M.S. Moorthy, J.-H. Bae, M.-J. Kim, S.-H. Kim and C.-S. Ha, *Part. Part. Syst. Charact*. 2013, **30**, 1044; b) Z. Tao, B.B. Toms, J. Goodisman and T. Asefa, *ACS Nano*. 2010, **4**, 789; c) M. Al-Shamsi, M.T. Al-Samri, S. Al-Salam, W. Conca, S. Shaban, S. Benedict, S. Tariq, A. Biradar, H.S. Penefsky, T. Asefa and A.-K. Souid, *Chem. Res. Toxicol*. 2010, **23**, 1796.

9 M. Manzano, V. Aina, C.O. Arean, F. Balas, V. Cauda, M. Colilla, M.R. Delgado and M. Vallet-Regi, *Chem. Eng.* 2008, **137**, 30.

10 a) F. Lin, M. Mettens, P. Cool and S.V. Doorslaer, *J. Phys. Chem. C*, 2013, **117**, 22723; b) E.D. Canck, I. Dosuna-Rodriguez, E.M. Gaigneaux and P. Van der Voort, *Materials*, 2013, **6**, 3556; c) G. Smeulders, V. Meynen, G.V. Baelen, M. Mertens, O.I. Lebeder, G.V. Tendeloo, B.U.W. Maes and P. Cool, *J. Mater. Chem*. 2009, **19**, 3042; d) C. Yoshina-Ishii, T. Asefa, N. Coombs, M.J. MacLachalan and G.A. Ozin, *Chem. Commun.* 1999, 2539.

11 a) J. Alanzun, A. Mehdi, C. Reye and R.J.P. Corriu, *J. Am. Chem. Soc*. 2006, **128**, 8718; b) R.K. Zeidan, S.J. Hwang and M.E. Devis, *Angew. Chem. Int. Ed*. 2006, **45**, 6332.

12 S.S. So and A.E. Mattson, *J. Am. Chem. Soc.* 2012, **134**, 8798.

13 Y.-L. Chang, M.-A. West, F.W. Fowler and J.W. Lauher, *J. Am. Chem. Soc*. 1993, **115**, 5991.

14 Q. Tang, Y. Xu, D. Wu and Y. Sun, *J. Solid. State. Chem*. 2006, **179**, 1513.

15 M.C. Bruzzoniti, A. Prelle, C. Sarzanini, B. Onida, S. Fiorilli and E. Garrone, *J. Sep. Sci*. 2007, **30**, 2414.

16 a) Q. Yang, S. Wang, P. Fan, L. Wang, Y. Di, K. Lin and F.-S. Xiao, *Chem. Mater*. 2005, **17**, 5999; b) H.-M. Kao, C.-H. Chung, D. Saikia, S.-H. Liao, P.-Y. Chao, Y.-H. Chen and K.C.-W. Wu, *Chem. Asian. J*. 2012, **7**, 2111; c) M. Xie, H. Shi, K. Ma, H. Shen, B. Li, S. Shen, X. Wang and Y. Jin, *J. Colloid. Interface. Sci*. 2013, **395**, 306.

17 C. Lei, Y. Shin, J. Liu and E.J. Ackerman, *J. Am. Chem. Soc*. 2002, **124**, 11242.

18 G. Wang, A.N. Otuonye, E.A. Blair, K. Denton, Z. Tao and T. Asefa, *J. Sol. State Chem.* 2009, **182**, 1649.

19 a) A.A. Gurinov, D. Mauder, D. Akcakayiran, G.H. Findenegg, I.G. Shendervich, *Chem. Phys. Chem.* 2012, **13**, 2282; b) H.-Y. Wu, F.-K. Shech, H.-M. Kao, Y.-H. Chen, J.R. Deka, S.-H. Liao, K.C.-W. Wu, *Chem. Eur. J*. 2013, **19**, 6358.

20 E.D. Canck, I. Ascoop, A. Sayari and P. Van Der Voort, *Phys. Chem. Chem. Phys*. 2013, **15**, 9792.

21 A. Szegedi, M. Popoval, I. Goshev and J. Mihaly, *J. Sol. State Chem*. 2011, **184**, 1201.

22 a) A. Datt, I. El-Maazawi and S.C. Larsen, *J. Phys. Chem. C*. 2012, **116**, 18358; b) B. Munoz, A. Ramila, J. Perez-Periente, I. Diaz and M. Vallet-Regi, *Chem. Mater*. 2003, **15**, 500.

23 a) J. March, Adv. Org. Chem. 3rd ed.; Wiley-Interscience: New York, 1985, 788; b) C.P. Wilgus, S. Downing, E. Molitor, S. Bains, R.M. Pagni and G.W. Kabalka, *Tetrahedron Letters.* 1995, **36**, 3469.

24 B. Kang, Z. Fu and S.H. Hong, *J. Am. Chem. Soc*. 2013, **135**, 11704.
25 G.-D. Fu, L.-Q. Xu, F. Yao, *J. Appl. Mater. Interface*, 2012, **1**, 2424.
26 Y.-S. Lin, C.-P. Tsai, H.-Y. Huang, C.T. Kuo, Y. Hung, D.-M. Huang, Y.-C. Chen and C.-Y. Mou, *Chem. Mater.* 2005, **17**, 4570.
27 J. Andersson, J. Rosenholm, S. Areva and M. Linden, *Chem. Mater.* 2004, **16**, 4160.
28 M. Manzano, V. Aina, C.O. Arean, F. Balas, V. Cauda, M. Colilla, M.R. Delgado and M. Vallet-Regi, *Chem. Eng. J.* 2008, **137**, 30.
29 J.J.E. Moreau, B.P. Pichon, M.C.W. Man, C. Bried, H. Pritzkow, J.L. Banfignies, P. Diudonne and J.L. Saunajol, *Angew. Chem. Int. Ed*. 2004, **13**, 203.
30 a) P.A. Kavakali, C. Uzun and O. Guven, *React. Funct. Polym*. 2001, **61**, 245; b) T. Caykara, S.S. Alaslan, M. Guru, H. Bodugoz and O. Guven, *Radiat. Phys. Chem*. 2007, **76**, 1569.
31 a) M. Xie, H. Shi, K. Ma, H. Shen, B. Li, S. Shen, X. Wang and J. Jin, *J. Colloid and Interface Sci.* 2013, **395**, 306; b) Z.-M. Cui, Z. Chen, C.-Y. Cao, L. Jiang and W.-G. Song, *Chem. Commun*. 2013, **49**, 2332.
32 S. Parambadath, V.K. Rana, D.Y. Zhao and C.S. Ha, *Micropor. Mesopor. Mater*. 2011, **141**, 94.
33 W. Whitenal, T. Asefa and G.A. Ozin, *Adv. Funct. Mater*. 2005, **15**, 1696.
34 L. Fu, R.A. Sa Ferreira, N.J.O. Silva, L.D. Carlos, V. de Zea Bermudez and J. Rocha, *Chem. Mater.* 2004, **16**, 1507.
35 H.-Y. Wu, F.-K. Shieh, H.-M. Kao, Y.-W. Chen, J.R. Deka, S.-H. Liao and K.C.-W. Wu, *Chem. Eur. J.* 2013, **19**, 6358.
36 a) K.Y. Ho, G. McKay and K.L. Yeung, *Langmur*, 2003, **19**, 3019; b) Q. Yang, S. Wang, P. Fan, L. Wang, Y. Di, K. Lin and F.-S. Xiao, *Chem. Mater*. 2005, **17**, 3999.
37 a) V.V. Guerrero and D.F. Shantz, *Ind. Chem. Eng. Res*. 2009, **48(23)**, 10375; b) L. Zhang, J. Liu, J. Yang, Q. Yang and C. Li, *Micropor. Mesopor. Mater*. 2008, **109**, 172.
38 I.I. Slowing, J.L. Vivero-Escoto, C.-W. Wu and V.S.-Y. Lin, *Adv. Drug Deliv. Rev*. 2008, **60**, 1278.
39 D. Lu, J. Lei, L. Wang and J. Zhang, *J. Am. Chem. Soc*. 2012, **134**, 8746.
40 a) T. Hekkila, H.J. Salonen, J. Tuura, N. Kumar, T.Y. Salmi, D.Y. Murzin, M.S. Hamdy, G. Mul L. Laitinen, A.M. Kaukonen, J. Hirvonen and V.P. Lehto, *Drug. Deliv.* 2007, **14**, 337; b) T. Higuchi, *J. Pharm. Sci*. 1963, **52**, 781.
41 a) M. Liong , J. Lu , M. Kovochich , T. Xia , S. G. Ruehm , A. E. Nel , F. Tamanoi and J. I. Zink, *ACS Nano*. 2008, **2**, 889; b) V. K. Rana, S. S. Park, S. Parambadath, M. J. Kim, S. Mishra, R. P. Singh and C. S. Ha , *Med. Chem. Commun*. 2011, **2**, 1162.
42 N. S. Rajinold, M. Muthunarayanan, K. P. Chennazhi, S. V. Nair and R. Jeyakumar, *Int. J. Biol. Macromol.* 2011, **48**, 98.
43 a) F. Babonneau, L. Yeung, N. Steunou, C. Gervais, A. Ramila and M. Vallet-Regi, *Mater. Res. Soc. Symp. Proc.* 2003, **775**, 3261; b) S.-W. Song, K. Hidajat and S. Kawi, *Langmuir,* 2005, **21**, 9568; c) F. Qu, G. Zhu, H. Lin, J. Sun, D. Zhang, S. Li and S. Qiu, *Eur. J. Inorg. Chem*. 2006, **19**, 3943.
44 a) Y.-F. Zhu, J.-L. Shi, Y.-S. Li, H.R. Chen, W.-H. Shen, X.-P. Dong, *Micropor. Mesopor. Mater*. 2005, **85**, 75; b) W. Zheng, X.-F. Qian, Y.-B. Zhang, J. Yin and Z.-K. Zhu, *Mater. Res. Bull*. 2005, **40**, 766.
45 T. Azais, C. Tourné-Péteilh, F. Aussenac, N. Baccile, C. Coelho, J.-M. Devoisselle, F. Babonneau, *Chem. Mater*. 2006, **18**, 6382.
46 W. Zeng, X.-F. Qian, J. Yin and Z.-K. Zhu, *Mater. Chem. Phys*. 2006, **97**, 437.
47 J.M. Rosenholm and M. Linden, *J. Control. Release*, 2008, **128**, 157.
48 a) B. Munoz, A. Ramila, J. Perez-Pariente, I. Diaz and M. Vallet-Regi, *Chem. Mater*. 2003, **15**, 500; b) S.W. Song, K. Hitajat and S. Kawi, *Langmuir,* 2005, **21**, 9568; c) F. Babonneau, L. Yeung, N. Steunou, C. Gervais, A. Ramila and M. Vallet-Regi, *Mater. Res. Soc*, 2003, **775**, 3261; d) Q. Tang, Y. Xu, D. Wu, Y. Sun, *J. Solid State Chem*. 2006, **179**, 1513.
49 a) W. Zeng, X.F. Qian, J. Yin and Z.K. Zhu, *Mater. Chem. Phys*, 2006, **97**, 437; b) W. Zheng, X.F. Qian, Y.B. Zhang, J. Yin and Z.K. Zhu, *Mater. Res. Bull*. 2005, **40**, 766.
50 a) F. Qu, G. Zhu, H. Lin, J. Sun, D. Zhang and S. Li, *Eur. J. Inorg. Chem*. 2006, **19**, 3943; b) J. Andersson, J. Rosenholm, S. Areva and M. Lindn, *Chem. Mater*. 2004, **16**, 4160.
51 S.K. Arya, K.C. Lee, D.B. Dah'alan, Danial and A.R.A. Rahman, *Lab Chip*, 2012, **12**, 2362.
52 H.N. Yehia, R.K. Draper, C. Mikoryak, E.K. Walker, P. Bajaj, I.H. Musselman, M.C. Daigrepont, G.R. Dieckmann and P. Pantano, *J. Nanobiotech*, 2007, 5:8, doi: 10.1186/1477-3155-5-8.
53 I.I. Slowing, B.G. Trewyn and V.S.Y. Lin, *J. Am. Chem. Soc*. 2006, **128**, 14792.

Table of content

The integrated nitrile groups into the pore walls of the mesoporous organosilica hybrids were converted into reactive carboxylic acid or amine groups, by acid or base hydrolysis techinique to achieve large amounts of either –COOH groups or –NH_2 groups into the pore walls. The *in vitro* drug release and biocompatibility tests proved the organosilica hybrids would be suitable drug carriers for both hydrophilic and hydrophobic drugs under an intracellular environment.